THERMAL STRUCTURE AND AEROSOL CONTENT OF THE MARTIAN ATMOSPHERE FROM TIRVIM-ACS ONBOARD TGO : AN OVERVIEW

S. Guerlet, S. Fan, F. Forget, E. Millour, *Laboratoire de Météorologie Dynamique/IPSL, Sorbonne Université, CNRS, Paris, France (sandrine.guerlet@lmd.ipsl.fr)*, **N. Ignatiev, P. Vlasov, A. Shakun, A. Trokhimovskiy, Oleg Korablev**, *IKI, Moscou, Russia,* **A. Grigoriev**, *ANU, Australia* and **F. Montmessin**, *LATMOS/IPSL, France*.

Introduction:

Between March 2018 and December 2019, millions of spectra of Mars' surface and atmosphere thermal emission have been recorded in nadir geometry by TIRVIM/ACS, a spectrometer onboard the ExoMars Trace Gas Orbiter (TGO). From this wealth of data, we characterized in detail the thermal structure and aerosol content in the Martian lower atmosphere at a great variety of local times. Indeed, TGO's orbit design is such that the local time of TIRVIM nadir observations drifted by 13 minutes earlier each sol. After 54 sols, a full coverage of the daily cycle was achieved along with excellent longitudinal and latitudinal coverage (up to 74° latitude due to TGO's inclination). This coverage allowed us to decompose thermal tides components at different seasons, to study the impact of the Global Dust Event of MY34 on the atmospheric and surface temperature, and to investigate the distribution of dust and water ice cloud optical depths. In this abstract, we review some of the main results obtained from TIRVIM data analysis and discuss them in light of comparisons to observations from the Mars Climate Sounder (MCS) and predictions from the LMD General Circulation Model.

Observations and Methods:

TIRVIM is a Fourier-transform spectrometer, part of the Atmospheric Chemistry Suite (ACS, Korablev et al., 2018), which started its operations on March 13, 2018. While TGO is still operational to this day, TIRVIM cryocooler stopped functioning in December, 2019. TIRVIM mostly operated in nadir geometry, where it recorded thermal emission of Mars' surface and atmosphere with sufficient signal-to-noise ratio between 600 and 1,300 cm^{-1} and a spectral resolution of 1.2 cm^{-1}.

We have developed an algorithm coupling line-by-line radiative transfer and optimal estimation theory to simultaneously retrieve, from TIRVIM nadir spectra, the surface temperature, the vertical profiles of the temperature between a few km and 50-55 km (2–3 Pa), and the integrated optical depth of dust and water ice clouds. The retrieved temperature profiles have a vertical resolution of typically 10 km (or one atmospheric scale height) in the lower atmosphere and an even coarser resolution of 15-20 km in the range 2–20 Pa. Temperature profiles retrieved from TIRVIM were validated against thousands of co-located observations from MCS. Those were acquired near 3AM and 3PM in limb viewing geometry with a better vertical coverage (5-80 km) and resolution (5 km). Once the differences in vertical resolution of the two instruments are taken into account, TIRVIM and MCS temperature profiles were found to agree within 2-3K in the range 300–2 Pa, which is highly satisfactory.

Details of our retrieval algorithm along with the MCS-TIRVIM cross-validation exercise can be found in Guerlet et al., 2022.

Thermal structure and tides:

Thermal tides are planetary-scale oscillations resulting from the diurnal solar forcing of the thin Martian atmosphere (eg., Zurek, 1976). They are responsible for most of the variation seen at the diurnal scale in atmospheric temperature or surface pressure data. In fact, they dominate the tropical climate. They are generally divided into migrating and non-migrating tides. The first category describes sun-synchronous modes propagating westward with the sun; the two main of these modes being the diurnal mode (with one maximum and one minimum per day and a zonal wavenumber of one) and the semi-diurnal mode (two maxima and two minima per day and a zonal wavenumber of two). Among the non-migrating tides, we can quote the eastward diurnal Kelvin waves or stationary waves.

One of the main advantage of TIRVIM observations is its full coverage of the diurnal cycle reached after 54 sols, or 25-35° of Ls, which allows to separate between diurnal and seasonal temperature variations. This is clearly an asset to study thermal tides compared to previous studies, mostly based on 2-4 AM and 2-4 PM temperatures obtained from sun-synchronous orbiters (eg., Guzewich 2012 and Kleinbohl et al., 2013 from MCS data and Banfield et al., 2000 and Wilson 2000 from TES observations).

An example of the zonally-averaged temperature retrieved from TIRVIM at 30 Pa in the period March 13 – April 28, 2018 (Ls~150° of MY34) is shown in Figure 1, as a function of latitude and local time. An instrumental issue occurred on April 28, limiting this first data set to 45 sols. Local time coverage is thus incomplete but represent roughly 80% of the martian day. Diurnal variations have a typical amplitude of 10K. Near the equator, the temperature is found maximum near 3~AM and minimum near 7~PM.

This feature of warm nighttime temperatures at this altitude is well known and is a manifestation of the diurnal thermal tide (Lee et al. 2009). The fact that these two temperature extrema are not separated by 12 hours is a first hint that the thermal field is also influenced by a semi-diurnal tide.

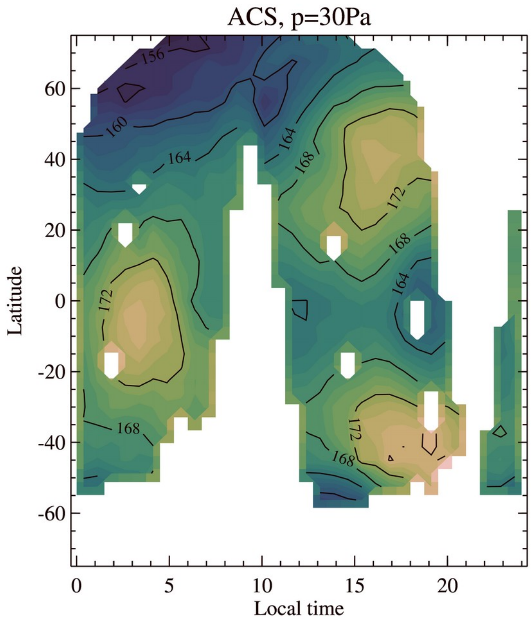

Figure 1: Zonally averaged temperature retrieved from TIRVIM/ACS at 30 Pa, with latitude and local time. This figure is obtained by gathering 45 sols of data around Ls~150°, MY34. Guerlet et al., in preparation.

To go beyond a qualitative analysis, we can study specifically the migrating tides by considering the zonally-averaged temperature in a fixed local time reference frame, in which other types of wave signatures (stationary waves, non-migrating tides,…) are averaged out. We assume that the zonally-averaged temperature at a given latitude and pressure level can be decomposed into a daily-averaged temperature plus two sinusoidal functions (at diurnal and semi-diurnal frequencies), following Kleinbohl et al., 2013. By fitting the observed temperatures, we thus derive the amplitude and phase of the diurnal and semi-diurnal migrating tides at each pressure level and for each 10°-wide latitudinal bin.

An example of such fits is shown for the equatorial region (between 5 and 5°) at Ls~150° of MY34. Regarding the diurnal mode, amplitudes of 4K are found near the equator, are only of 2K near 20°, and increase to 6K near 50°N (Guerlet et al., in preparation). Very similar results are found at Ls~90° for MY35 (Fan et al., 2022). Our results agree well with previous studies, providing that the rather coarse vertical resolution of TIRVIM nadir observations is taken into account. We employ the same methodology to derive tides characteristics simulated in the LMD Global Circulation Model, run using the MY34 dust scenario (Montabone et al., 2020). Temperature profiles from the GCM are extracted at the same locations and times as TIRVIM observations, and are smoothed vertically using the appropriate averaging kernel matrix. We find that the GCM exhibits migrating tides with very similar characteristics as those observed, except for a 1 to 2 hours phase shift; temperature extrema occurring at later local times in the model.

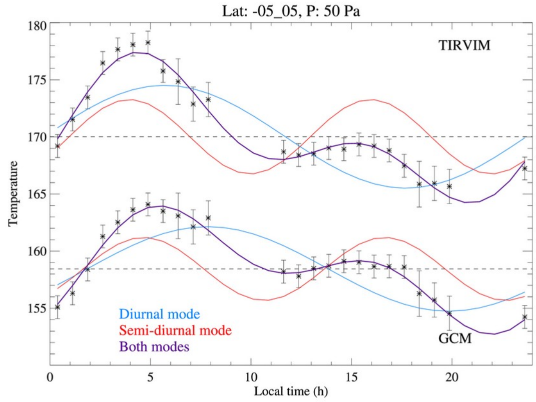

Figure 2: Example of a fit (purple) to TIRVIM equatorial temperatures at 50 Pa (black stars, upper part) as a function of local time. The fit combines a daily average temperature (horizontal dashed line); diurnal and semi-diurnal signals, as labeled. The bottom part shows the same for GCM outputs (shifted by -15K). Note that a seasonal detrending was applied to the data. Guerlet et al., in preparation.

One caveat is that seasonal variations over a martian month, although of small amplitude, can hamper our analysis when characterizing the semi-diurnal tide. Indeed, as TIRVIM samples the atmosphere twice per day, an overall seasonal warming (for instance) over the course of 54 sols could be wrongly interpreted as warming with local time, occurring twice per day (Fan et al., 2022). To overcome this issue, we de-trend the data for seasonal variations using MCS observations (Guerlet et al., in preparation). The derived amplitude of the semi-diurnal tide near the equator at Ls=150° ranges from 2K (at 100 Pa) to 6K (at 2 Pa), confirming that this tide mode is significant even in non-dusty seasons (Kleinbohl et al., 2013).

We can also exploit the full longitude-time coverage of TIRVIM observations to search for signatures of both migrating and non-migrating tides. This approach was employed by Fan et al., 2022 for the analysis of TIRVIM data acquired around Ls=90° of MY35. A diurnal Kelvin wave was detected with an amplitude of 2.5K at 200 Pa, well reproduced in the GCM.

Dust distribution and impact of the MY34 GDE: A Global Dust Event started locally on 2 June 2018 (Ls=186° of MY34) and reached a mature phase on 21 June (Ls=197°), when it became planet-encircling (Kass et al., 2020).

Dust storms are known to cause warmer nighttime surface temperatures and colder daytime surface temperatures. This was well observed with TIRVIM, with day-night temperature contrasts reduced to ~20-30K during the MY34 GDE, instead of ~80-90K just before the onset of the storm (Pavel et al., submitted).

Retrieving dust optical depth from nadir sounding can be challenging, especially when the contrast between surface and atmospheric temperature (in the region where most of the dust lies) is low. Systematic biases in dust column retrievals can also occur due to wrong assumptions in the dust vertical distribution (Guerlet et al., 2022). We present below two examples of latitude/longitude distribution of dust opacities obtained by averaging day and night measurements: one shortly after the onset of the storm, the other during the mature phase of it. The morphology of the dust spatial distribution matches well, qualitatively, that derived by extrapolating MCS dust profiles (Montabone et al., 2020). Similar results were obtained by Pavel et al. (submitted). Further work is needed to improve these retrievals and better study their diurnal cycle.

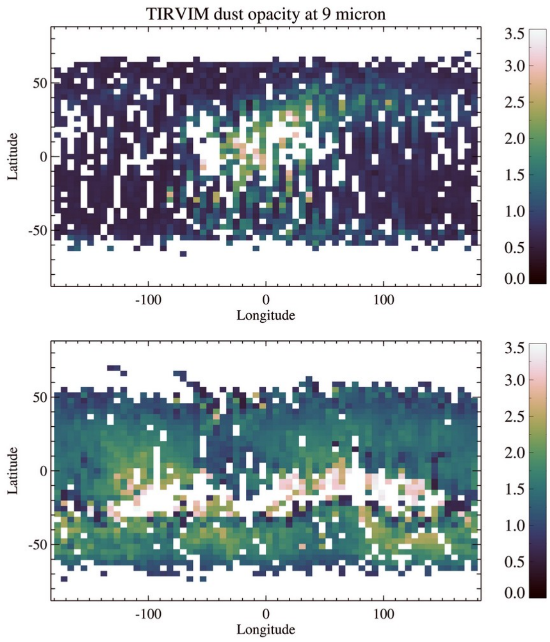

Figure 3: Dust column opacity retrieved on 6-10 June (top) and on 4-9 July 2018 (bottom).

We can also estimate the thermal tides amplitudes and phases during the storm thanks to the extended local time coverage of TIRVIM data. However, this is a challenging task, as the thermal structure of the atmosphere changes significantly over timescales of ~10-15° degrees of Ls, even during the mature phase of the storm. We thus focus on only 15 sols (21 June – 6 July) covering local times from 5 to 9AM, and combine these observations to MCS ones acquired the same dates but at ~3AM and ~3PM. Compared to pre-storm conditions, we find that the diurnal tide amplitude strongly increases during the storm, reaching 32K at 50-60°S and 20K at 50-60°N at 50 Pa, while it remains unchanged (~4K) near the equator. The semi-diurnal mode increases slightly (6-8K at 30-50 Pa, equator), while the ter-diurnal mode is also detected (amplitude of 5K near 50 Pa, equator). GCM simulations run with the MY34 dust scenario (itself based on MCS dust observations) agree very well with TIRVIM observations, both in terms of thermal structure and tide characteristics.

TIRVIM atmospheric temperatures and dust column opacities retrieved during the GDE have also been successfully used in a data assimilation scheme (see MAMO abstract by R. Young et al). Assimilation of all TIRVIM data is in progress and should lead to the distribution of a reanalysis, a reference atmospheric state (temperature but also wind fields, etc).

Water ice distribution: Retrieving total column water ice opacity is also challenging, mainly because of the unknown vertical distribution of clouds. This can strongly bias their retrieved opacity from TIRVIM (Guerlet et al., 2022). However, preliminary results are encouraging. We show below the evolution of water ice total column opacity with local time retrieved during aphelion season (Ls~90° of MY35). Significant scatter in the retrieved values can be noted at night, but a trend of minimum cloud opacity at midday (10h-15h) is clearly visible. Refining our a priori knowledge on the water ice vertical distribution (based for instance on independent limb measurements from MCS and occultations by ACS) needs to be done to continue investigating cloud opacities at different local times.

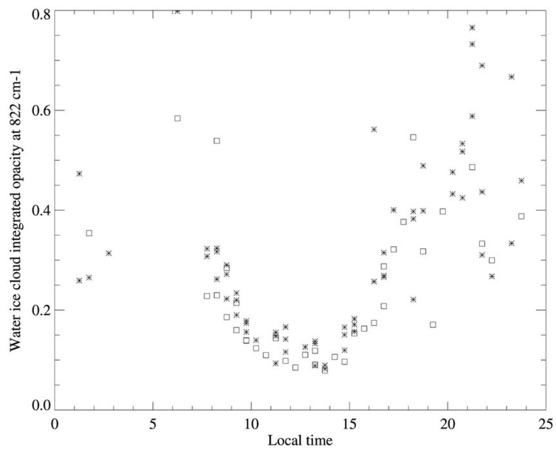

Figure 4: Water ice cloud opacity as a function of local time, over the range 25°N-25°S at Ls~90° of MY35.

Conclusion: Millions of atmospheric temperature profiles have been retrieved from ACS/TIRVIM nadir observations. A selection of these profiles has been cross-validated with MCS limb retrievals with a high level of correspondence. From these profiles, we can study the full diurnal cycle of temperature by gathering data over a martian month. Migrating and non-migrating tide amplitudes and phases can be derived with greater accuracy than with sun-synchronous orbiters, with the caveat of a rather coarse vertical resolution. Our results are in good agreement with predictions from the General Circulation Model, although some differences are found in the tide phases, calling for further model developments. Seasonal changes over a month can impact our results on the semi-diurnal migrating tide, but this issue can be addressed by de-trending TIRVIM data using independent measurements. The Global Dust Event of 2018 completely modified the tide structure, with a very large amplitude of the diurnal mode of 32K found at 50 Pa at 50-60°S, and an enhancement of the semi and ter-diurnal tide found at the equator. As expected, day/night surface temperature contrasts are severely reduced during the storm. Total integrated dust columns retrieved from TIRVIM seem qualitatively consistent with dust columns extrapolated from MCS, although outliers are present. Our retrievals were also successfully used in a data assimilation scheme. Future work will focus on refining aerosol retrievals by using more appropriate assumptions on their vertical distribution. Current version of TIRVIM retrievals (corresponding to the algorithm describe in Guerlet et al., 2022) are available in NetCDF format at:
https://doi.org/10.14768/ab765eba-0c1d-47b6-97d6-6390c63f0197

Bibliography:

Banfield et al., JGR Vol. 105, 2000.
Fan et al., GRL Vol. 49, 2022.
Guerlet et al., JGR Vol. 127, 2022.
Guzewich et al., JGR Vol. 117, 2012.
Kass et al., GRL Vol. 47, 2020.
Kleinbohl et al., GRL Vol. 40, 2013.
Korablev et al., SSR Vol. 214, 2018.
Lee et al., JGR Vol. 114, 2009.
Montabone et al., JGR Vol. 125, 2020.
Pavel et al., *submitted to JGR.*
Wilson et al., GRL Vol. 27, 2000.
Zurek, JAS Vol. 33, 1976.